SNORD3B-2, close paralogues of U3 snoRNA, guide site specific cleavage of rRNA during pre-rRNA processing.[10] We report *SNORD3B-1* and *SNORD3B-2* are upregulated in bone cancer (Table 1). *SNORD58B* is reported to guide the 2′-O-methylation of residue G4198 of the 28S rRNA.[11] We found *SNORD58B* was downregulated in our bone cancer samples (Table 1).

RNA therapeutics are on the horizon. LncRNA and snoRNA are of recent interest because of their elusive roles in regulating gene expression and epitranscriptomic modification of pre-RNAs. RNA is also a specific biomarker, which is especially helpful in providing a robust diagnosis in rare and heterogeneous cancers. Bone cancers are historically difficult to diagnose and subclassify prior to surgery, which can delay the appropriate choice of neoadjuvant chemotherapeutic agents. *H19* expression after birth is linked to Beckwith–Wiedemann syndrome, which increases the likelihood of childhood cancer but not adult cancer. We found that *H19-203* may be a specific biomarker for osteosarcomas involving *SHH* signalling. Patients may benefit from receiving targeted *SHH* inhibitors sonidegib or vismodegib that are currently used to treat basal cell carcinoma. We also found low *MEG3-224* and high *XIST-201/XIST-204* may be markers of poor prognosis and lower overall survival in patients, which we detected in two of four patients. Upregulation of snoRNAs is consistent with the increased proliferative behaviour of cancer cells. *SNORD68*, *SNORD3B-1* and *SNORD3B-2* may be useful biomarkers in the future. Previous research has shown the *EWSR1-FLI1* chimaeric transcript in Ewing sarcoma is sensitive to snoRNA loss of function due to changes in splicing, demonstrating a potential target for intervention in Ewing sarcoma cells through snoRNA activity.[12]

A limitation of this study is the size of the cohort studied. Bone cancer is rare and donation to tissue banks is scarce. Our data highlight the value of being able to provide a specific tissue diagnosis in addition to identifying regulatory transcriptomic molecules that could be exploited for targeted therapy.

Acknowledgements: Approval to obtain and study human tissue was granted by the Faculty of Medicine and Health Sciences Research Ethics Committee (2015/16 100 HT). The cancer data presented in this study is publicly available on GEO under the accession GSE113916. The control data used in this study is publicly available on GEO under the accession GSE55282. We thank Lucy Bishton, Natalie Jackson, Dionne Wortley, Kulvinder Jill and Karen Joynes (The Royal Orthopaedic Hospital) for supporting collection of patient samples.

Conflicts of interest and sources of funding: This study was funded by The Humane Research Trust. The authors state that there are no conflicts of interest to disclose.

Darrell Green[1], Archana Singh[2], Jasmine Sanghera[2], Lee Jeys[3], Vaiyapuri Sumathi[4], Tamas Dalmay[2], William D. Fraser[1,5]

[1]Norwich Medical School, University of East Anglia, Norwich Research Park, Norwich, United Kingdom; [2]School of Biological Sciences, University of East Anglia, Norwich Research Park, Norwich, United Kingdom; [3]Department of Orthopaedic Oncology, The Royal Orthopaedic Hospital, Birmingham, United Kingdom; [4]Department of Musculoskeletal Pathology, The Royal Orthopaedic Hospital, Birmingham, United Kingdom; [5]Department of Clinical Biochemistry, Norfolk and Norwich University Hospital, Norwich Research Park, Norwich, United Kingdom

Contact Prof William D. Fraser.
E-mail: W.Fraser@uea.ac.uk

1. Green D, Dalmay T, Fraser WD. Role of miR-140 in embryonic bone development and cancer. *Clin Sci (Lond)* 2015; 129: 863–73.
2. Rojas-Pena ML, Olivares-Navarrete R, Hyzy S, *et al*. Characterization of distinct classes of differential gene expression in osteoblast cultures from non-syndromic craniosynostosis bone. *J Genomics* 2014; 2: 121–30.
3. Pertea M, Kim D, Pertea GM, *et al*. Transcript-level expression analysis of RNA-seq experiments with HISAT, StringTie and Ballgown. *Nat Protoc* 2016; 11: 1650–67.
4. Bray NL, Pimentel H, Melsted P, *et al*. Near-optimal probabilistic RNA-seq quantification. *Nat Biotechnol* 2016; 34: 525–7.
5. Raveh E, Matouk IJ, Gilon M, *et al*. The H19 long non-coding RNA in cancer initiation, progression and metastasis – a proposed unifying theory. *Mol Cancer* 2015; 14: 184.
6. Chan LH, Wang W, Yeung W, *et al*. Hedgehog signaling induces osteosarcoma development through Yap1 and H19 overexpression. *Oncogene* 2014; 33: 4857–66.
7. Tian ZZ, Guo XJ, Zhao YM, *et al*. Decreased expression of long non-coding RNA MEG3 acts as a potential predictor biomarker in progression and poor prognosis of osteosarcoma. *Int J Clin Exp Pathol* 2015; 8: 15138–42.
8. Mao H, Wang K, Feng Y, *et al*. Prognostic role of long non-coding RNA XIST expression in patients with solid tumors: a meta-analysis. *Cancer Cell Int* 2018; 18: 34.
9. Liang L, Xu J, Wang M, *et al*. LncRNA HCP5 promotes follicular thyroid carcinoma progression via miRNAs sponge. *Cell Death Dis* 2018; 9: 372.
10. Clery A, Senty-Segault V, Leclerc F, *et al*. Analysis of sequence and structural features that identify the B/C motif of U3 small nucleolar RNA as the recognition site for the Snu13p-Rrp9p protein pair. *Mol Cell Biol* 2007; 27: 1191–206.
11. Kiss-Laszlo Z, Henry Y, Bachellerie JP, *et al*. Site-specific ribose methylation of preribosomal RNA: a novel function for small nucleolar RNAs. *Cell* 1996; 85: 1077–88.
12. Grohar PJ, Kim S, Rangel Rivera GO, *et al*. Functional genomic screening reveals splicing of the EWS-FLI1 fusion transcript as a vulnerability in Ewing sarcoma. *Cell Rep* 2016; 14: 598–610.

DOI: https://doi.org/10.1016/j.pathol.2018.08.014

Rhabdomyosarcoma with *FUS* re-arrangement: additional case in support of a novel subtype

Sir,

The World Health Organization (WHO) Classification of Bone and Soft Tissue Tumours currently recognises four subcategories of rhabdomyosarcoma, namely, embryonal, alveolar, pleomorphic and spindle cell/sclerosing subtypes.[1] Each is characterised by specific and well-described clinical, morphological and molecular features. Very recently, a novel, rare and molecularly-defined subtype of rhabdomyosarcoma has been identified from RNA sequencing of a series of previously unclassified ‘small round cell sarcomas’.[2] These tumours have in common a highly aggressive biological course, monomorphic epithelioid and spindle cell morphology and the unusual combination of ALK protein over-expression and a defining *FUS* (or *EWSR1*)-*TFCP2* fusion.

In this report, we describe the fifth case of this rare sarcoma and demonstrate for the first time the presence of a large *ALK*

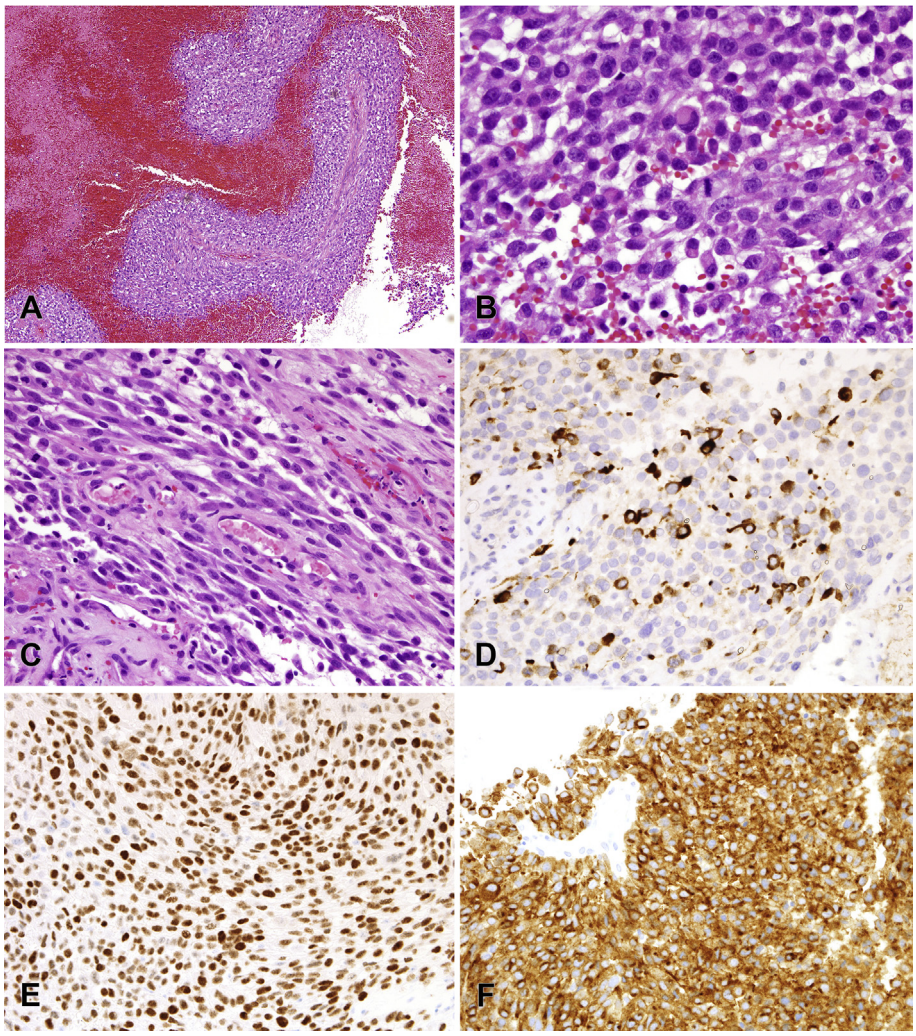

Fig. 1 Rhabdomyosarcoma with *FUS* re-arrangement. (A) The tumour was extensively necrotic and haemorrhagic, sparing perivascular cuffs of mitotically active malignant cells, with (B) mixed epithelioid and rhabdoid, as well as (C) spindle cell morphology. (D) Immunohistochemistry showed patchy staining for desmin and (E) diffuse staining for MyoD1 and (F) ALK.

gene deletion suggesting that the observed ALK protein over-expression likely represents a truncated isoform.

A 23-year-old male presented with nasal congestion, found to be related to a left nasal cavity tumour which had rapidly grown in size to 80 mm over 4 months as seen on serial imaging. Staging positron emission tomography-computed tomography (PET-CT) showed the mass to be highly FDG-avid with no metastases or occult primary sites of disease elsewhere. A trans-nasal biopsy was performed, comprising multiple pieces of an extensively necrotic malignant tumour with a peritheliomatous growth pattern (Fig. 1). Confluent areas of necrosis spared perivascular cuffs of monomorphic epithelioid, rhabdoid and some plump spindle cells, surrounding rounded thin- and thick-walled vessels. The cells demonstrated large and mildly pleomorphic nuclei with coarse chromatin, variably prominent nucleoli and moderate volumes of eosinophilic cytoplasm, sometimes forming globular inclusions. Rhabdomyoblasts with cross-striations did not feature. Mitotic activity was brisk with >30 mitoses counted per 10 high power fields (field area 0.23 sq mm).

Immunohistochemistry showed strong and diffuse staining for MyoD1 with patchy staining for desmin and isolated co-expression of myogenin (Fig. 1). There was also strong cytoplasmic staining for ALK1 (ALK01 clone) and diffuse membranous staining for CD99. Negative stains included AE1/AE3, MNF116, CK8/18, CK7, CK20, EMA, S100, SOX10, HMB45, CD34, STAT6, ERG, WT1, NKX2-2, ETV4, CD56 and CD117. INI1 expression was retained.

Interphase FISH analysis demonstrated a *FUS* (16p11) re-arrangement in 35% of cells examined. An *ALK* (2p23) disruption was also observed in 80% of cells in which there was retention of the red 3′ signal and loss of the green 5′ signal (Fig. 2). There was no re-arrangement of *DDIT3* (12q13), *EWSR1* (22q12), *CREB1* (2q33) or *ATF1* (12q13) genes and no evidence of a *PAX3-FOXO1* or *PAX7-FOXO1* fusion. Next generation sequencing was also performed using the TruSight Tumour 170 panel (Illumina, USA) showing an apparent large *ALK* gene deletion with RNA splicing corresponding to skipping of exons 1−16. The list of fusions detected by the platform did not include *FUS* and therefore the panel was unable to confirm the *FUS* re-arrangement seen on FISH analysis nor identify the partner gene.

The findings overall were entirely consistent with the novel rhabdomyosarcoma subtype only recently reported by

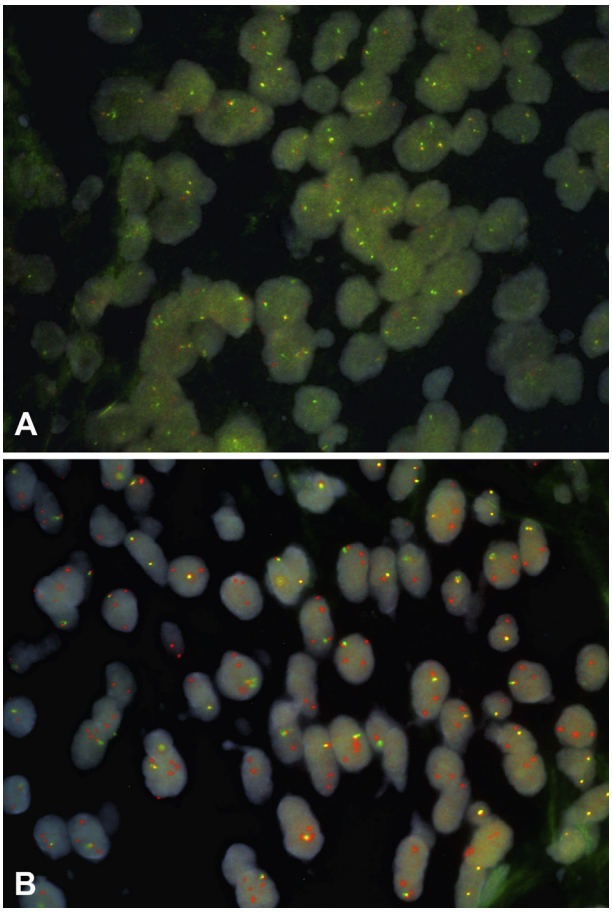

Fig. 2 (A) Interphase FISH analysis showed a pattern consistent with a *FUS* re-arrangement, with separation of the red 5′ and green 3′ signals in 35% of cells examined. (B) There was also a pattern indicating an *ALK* disruption, with the red 3′ signal visualised without the accompanying green 5′ signal in 80% of cells. This corresponds to the large *ALK* gene deletion detected on next generation sequencing involving exons 1−16.

Watson *et al.*[2] with *FUS* re-arrangement and ALK over-expression, the latter shown in this case to likely represent a truncated isoform in the presence of large *ALK* gene deletion. The patient is presently being treated with the ALK inhibitor, crizotinib, after failing to respond to conventional combination chemotherapy and radiotherapy.

The current WHO classification recognises four subtypes of rhabdomyosarcoma.[1] Embryonal rhabdomyosarcoma is the most common, typically occurring in the head and neck and genitourinary tract of children. Histologically, these tumours are composed of spindled and stellate cells randomly dispersed within a myxoid stroma, classically with subepithelial condensation at mucosal sites (so-called 'cambium layer'). A complex karyotype is observed with typical loss of heterozygosity at 11p15.5.[3] Alveolar rhabdomyosarcoma affects adolescents and young adults, most commonly in the deep soft tissues of the extremities and is a small round cell sarcoma, associated with either a *PAX3-FOXO1* or *PAX7-FOXO1* fusion.[3] Pleomophic rhabdomyosarcoma is a sarcoma of adults, also affecting the deep soft tissues of the extremities, with a complex karyotype and without recurring single genetic events.[4] More recently, spindle cell/sclerosing rhabdomyosarcoma has been separated from embryonal rhabdomyosarcoma as a distinct entity.[1] The spindle cell subtype appears to differ in its molecular features according to age, with those occurring in young children showing fusions involving either *NCOA2* or *VGLL*,[5,6] and those occurring in older children and adults showing mutations of *MYO-D1*.[7] Sclerosing rhabdomyosarcoma is thought to represent a related entity along the same morphological spectrum, sharing in common mutations of *MYO-D1* and less commonly, *PIKC3A*.[5,7]

In early 2018, Watson *et al.*[2] reported a novel and distinct subtype of rhabdomyosarcoma based on three cases identified from RNA sequencing of several cohorts of previously unclassified 'small round cell sarcomas'. Subsequent to this, a further case was reported by Dashti *et al.*[8] The clinicopathological features of the five cases now described (including the current case) are summarised in Table 1. In brief, these tumours preferentially occur in young adults (median age 26 years), although with a wide age range (16−72 years). Males and females are affected approximately equally and the tumours arise in a wide variety of sites including bone and soft tissue. They pursue a highly aggressive clinical course, with no patients surviving beyond 5 months in the three cases originally reported.[2]

Morphologically, these tumours are composed of a relatively monomorphic population of epithelioid, spindled and rhabdoid cells occurring in sheets. The cells demonstrate mildly pleomorphic nuclei with prominent nucleoli and moderate volumes of eosinophilic cytoplasm. Mitotic activity is brisk and necrosis is frequent, often producing a peritheliomatous growth pattern. Rhabdomyoblasts with cross-striations do not feature. The relative proportion of epithelioid and spindled cells is variable and explains the discrepancy between the original study by Watson *et al.* in which the tumour is described as an 'epithelioid rhabdomyosarcoma'[2] and the subsequent single case report by Dashti *et al.* in which it is described as a 'spindle cell rhabdomyosarcoma'.[8] Like other rhabdomyosarcomas, these tumours express desmin, myogenin and Myo-D1 (as well as occasional aberrant staining for cytokeratins), although myogenin expression is more limited and can be restricted to isolated cells. However, of interest in this entity is over-expression of ALK, initially identified through gene expression profiling[2] but routinely demonstrable with the commonly used ALK01 antibody on immunohistochemistry where it produces a cytoplasmic pattern of reactivity.[8]

The molecular signature of this new subtype is a fusion involving either *FUS* (16p11) or *EWSR1* (22q12), which pairs with the *TFCP2* (12q13) gene. Although the partner

Table 1 Summary of published cases of *FUS/EWSR1*-rearranged rhabdomyosarcoma

Reference	Age (yrs)	Sex	Site	Fusion	Follow-up
Watson *et al.*[2]	38	F	Chest wall	*EWSR1-TCFP2*	DOD <5m
Watson *et al.*[2]	26	F	Pelvic bone	*FUS-TFCP2*	DOD <5m
Watson *et al.*[2]	16	F	Sphenoid bone	*FUS-TFCP2*	DOD <5m
Dashti *et al.*[8]	72	M	Mandible	*FUS-TCP2*	AWOD 2m
Current	23	M	Nasal cavity	*FUS* fusion	AWD 2m

AWD, alive with disease; AWOD, alive without disease (post-surgery without adjuvant therapy); DOD, dead of disease; m, months.

gene of the *FUS* re-arrangement was not confirmed in our case, the overall clinicopathological features (including ALK over-expression) are such that the tumour almost certainly corresponds to this new entity. Herein, we also present the previously unreported finding that ALK over-expression in these sarcomas likely represents a truncated isoform lacking part of, or the entire, extracellular domain of the receptor tyrosine kinase. This is inferred based on detection of a large *ALK* gene deletion involving exons 1−16 using next generation sequencing. The deletion corresponds to the diffuse loss of the 5′ green signal observed on interphase FISH analysis. Immunohistochemical detection of the truncated protein is retained given that the commonly used, commercially available ALK antibodies (including ALK01 and D5F3) are directed against the preserved C-terminus. The exact mechanism of protein over-expression in this tumour remains unclear although may be explained by a splice variant or novel fusion.

The findings bring forth several interesting possibilities for the medical treatment of these biologically aggressive sarcomas. ALK over-expression suggests that these tumours may respond to ALK inhibitors such as crizotinib although it is uncertain whether the absence of the extracellular domain in the expressed truncated protein may limit the effectiveness of the drug. There is some evidence to suggest that ALK inhibitors do retain their efficacy in this setting, albeit reduced compared to tumours with genuine *ALK* fusions.[9] The *TFCP2* gene also codes for a transcription factor which upregulates thymidylate synthetase, the rate limiting enzyme responsible for the production of dTTP, critical for DNA synthesis.[10] Thymidylate synthetase is inhibited by the well-established chemotherapeutic agent, 5-fluorouracial (5-FU), which therefore may also have a role in therapy. However, it is yet to be determined whether these theoretical considerations will translate to 'real world' outcomes, including for the patient described in this report presently being treated with crizotinib.

The differential diagnosis of this novel rhabdomyosarcoma is broad, and in part depends on the variable proportion of epithelioid, spindled and rhabdoid cells as well as whether the tumour is arising primarily within bone or soft tissue. Poorly-differentiated/sarcomatoid carcinoma (with or without heterologous rhabdomyoblastic differentiation) and malignant melanoma require exclusion in the first instance, together with other recognised subtypes of rhabdomyosarcoma described earlier (Of note, in 2011, Jo *et al.*[11] described a morphological variant of rhabdomyosarcoma which they termed 'epithelioid rhabdomyosarcoma', which is not currently recognised by the WHO classification.[1] *FUS* and *EWSR1* re-arrangements were not tested for as part of this study. The relationship between these tumours and the novel subtype of rhabdomyosarcoma described herein is unclear, although there is likely to be overlap.) Other sarcomas that also merit consideration include malignant myoepithelioma, atypical Ewing sarcoma, malignant peripheral nerve sheath tumour (with heterologous rhabdomyoblastic differentiation), epithelioid sarcoma and leiomyosarcoma. However, the unusual combination of myogenin, MyoD1 and ALK (over-) expression with *FUS* (or *EWSR1*) re-arrangement is sufficiently distinctive to establish the diagnosis and exclude the aforementioned diagnostic possibilities.

In summary, we present the fifth case of a rare subtype of rhabdomyosarcoma, lending support to the existence of a new and distinctive clinicopathological entity. In addition to re-affirming the variable epithelioid, spindled and rhabdoid morphology and characteristic *FUS* (or *EWSR1*) re-arrangement, we report the novel finding that the previously described ALK over-expression in these tumours likely represents a truncated isoform occurring in the presence of a large *ALK* gene deletion. Further cases are awaited to refine the clinicopathological features and prognosis, as well as to determine whether they might respond to targeted therapies such as ALK inhibitors.

Acknowledgements: The authors would like to acknowledge Prof Jason Hornick, Brigham and Women's Hospital, Boston, for reviewing the case and A/Prof Ravindra Kolhe, Medical College of Georgia, Augusta, for reviewing the next generation sequencing data. We would also like to acknowledge the Departments of Diagnostic Genomics and Molecular Pathology, PathWest, QEII Medical Centre, for the FISH and the next generation sequencing analysis, respectively.

Conflicts of interest and sources of funding: The authors state that there are no conflicts of interest to disclose.

Daniel D. Wong[1,2], Chris van Vliet[1], Andrew Gaman[3], Tindaro Giardina[1], Benhur Amanuel[1]

[1]Department of Anatomical Pathology, PathWest, QEII Medical Centre, Nedlands, WA, Australia; [2]School of Pathology and Laboratory Medicine, The University of Western Australia, Crawley, WA, Australia; [3]Department of Anatomical Pathology, CliniPath Pathology, Osborne Park, WA, Australia

Contact Dr Daniel D. Wong.
E-mail: daniel.wong@health.wa.gov.au

1. Fletcher CD, Bridge JA, Hogendoorn PCW, *et al*. *WHO Classification of Tumours of Soft Tissue and Bone*. 4th ed. Lyon: IARC, 2013.
2. Watson S, Perrin V, Guillemot D, *et al*. Transcriptomic definition of molecular subgroups of small round cell sarcomas. *J Pathol* 2018; 245: 29−40.
3. Davicioni E, Anderson MJ, Finckenstein FG, *et al*. Molecular classification of rhabdomyosarcoma—genotypic and phenotypic determinants of diagnosis: a report from the Children's Oncology Group. *Am J Pathol* 2009; 174: 550−64.
4. Li G, Ogose A, Kawashima H, *et al*. Cytogenetic and real-time quantitative reverse-transcriptase polymerase chain reaction analyses in pleomorphic rhabdomyosarcoma. *Cancer Genet Cytogenet* 2009; 192: 1−9.
5. Alaggio R, Zhang L, Sung YS, *et al*. A molecular study of pediatric spindle and sclerosing rhabdomyosarcoma: identification of novel and recurrent VGLL2-related fusions in infantile cases. *Am J Surg Pathol* 2016; 40: 224−35.
6. Mosquera JM, Sboner A, Zhang L, *et al*. Recurrent NCOA2 gene rearrangements in congenital/infantile spindle cell rhabdomyosarcoma. *Genes Chromosomes Cancer* 2013; 52: 538−50.
7. Agaram NP, Chen CL, Zhang L, *et al*. Recurrent MYOD1 mutations in pediatric and adult sclerosing and spindle cell rhabdomyosarcomas: evidence for a common pathogenesis. *Genes Chromosomes Cancer* 2014; 53: 779−87.
8. Dashti NK, Wehrs RN, Thomas BC, *et al*. Spindle cell rhabdomyosarcoma of bone with FUS-TFCP2 fusion: confirmation of a very recently described rhabdomyosarcoma subtype. *Histopathology* 2018; 73: 514−20.

9. Gao X, Sholl LM, Nishino M, *et al*. Clinical implications of variant ALK FISH rearrangement patterns. *J Thorac Oncol* 2015; 10: 1648−52.
10. Powell CM, Rudge TL, Zhu Q, *et al*. Inhibition of the mammalian transcription factor LSF induces S-phase-dependent apoptosis by downregulating thymidylate synthase expression. *EMBO J* 2000; 19: 4665−75.
11. Jo VY, Marino-Enriquez A, Fletcher CD. Epithelioid rhabdomyosarcoma: clinicopathologic analysis of 16 cases of a morphologically distinct variant of rhabdomyosarcoma. *Am J Surg Pathol* 2011; 35: 1523−30.

DOI: https://doi.org/10.1016/j.pathol.2018.09.056

Uterine intravascular adenomyomatosis: a bizarre hybrid lesion?

Sir,

Uterine adenomyosis is a common pathological entity and very familiar to histopathologists. Less familiar and probably under-recognised is the presence of an intravascular component to the process which occurs in 12−18% of cases, and largely confined to instances of 'deep' adenomyosis. Benign uterine leiomyomas are, if anything, even more frequently encountered than adenomyosis and once again local intrusion ('invasion') into vascular spaces may be seen, usually at or within the margins of the leiomyoma. As with intravenous adenomyosis, this is of no clinical consequence. Rarely, more extensive and often macroscopically visible intravascular invasion is encountered. This quasi-malignant neoplastic process of intravenous or intravascular leiomyomatosis (IVL) with tongues of benign-appearing smooth muscle in large venous and lymphatic spaces within the myometrium shares molecular changes such as der (14)t (12; 14) (q15; q24) with ordinary uterine leiomyomas,[1] and expression profiles that more closely resemble those of leiomyosarcomas.[2]

While seemingly quite separate and pathogenetically unrelated entities, we have encountered an example of a recently described hybrid of intravascular adenomyosis and leiomyomatosis, which displays morphological features of both and which has been termed intravascular adenomyomatosis.[3] These authors reported five cases, four of which had follow up information with no recurrences, as was also the case in a subsequently published case.[4] Only one of the original five cases had extrauterine extension (of intravascular leiomyomatosis). All six cases had histological evidence of uterine adenomyosis and in four examples, the intravascular adenomyomatous component was in close proximity to the adenomyosis, while in two cases it was remote. All six cases also had benign leiomyomas (including one cellular leiomyoma) but the spatial relationship between the leiomyomas and the intravascular component was less clearly described.

Our case was a 48-year-old woman with no significant past medical history, who underwent a subtotal hysterectomy for severe menorrhagia and polymenorrhoea. The uterine body weighed 256 g and measured 110 × 100 × 70 mm. The myometrium was coarsely trabeculated and included three poorly circumscribed mural tan nodules with partly whorled cut surfaces, 12−28 mm in maximum dimensions, and multiple further well defined pale whorled mural nodules 1−2 mm across. Some of the latter displayed central spaces and the overall appearances were typical of florid deep adenomyosis. Occasional circumscribed leiomyomas were also seen.

Histological examination showed normal secretory endometrium and confirmed the presence of several small benign leiomyomas as well as extensive conventional adenomyosis. The 28 mm mural nodule and the smaller ones adjacent to it, by contrast, were complex and haphazard aggregations of discrete islands of entirely unremarkable adenomyosis (mostly with stroma and glands but sometimes stroma only) and tongues of intravascular extension, all within hypertrophied myometrial smooth muscle. About one-third of these intravascular extensions were characterised by typical endometrial stroma only while the remainder exhibited variable mixtures of endometrial type stroma and glands (Fig. 1A), vascular smooth muscle tissue (Fig. 1B) or all three (Fig. 1C). Some intravascular extensions were seen as apparently free-floating, but presumably pedunculated, intravascular islands (Fig. 1D) while others were more obviously attached to the vessel wall by a broad stalk or pedicle and a few were merely sub-endothelial plaques. Numerous transitions between islands of deep adenomyosis and intravascular extensions were present. This phenomenon did not involve the superficial islands of adenomyosis present in the inner third of the myometrium, nor the scattered small benign leiomyomas, even those intravascular extensions that were purely smooth muscle in differentiation. An unusual variation on the general theme was a large solitary intravascular plug composed of an intimate admixture of endometrial type stroma and glands and vascular smooth muscle (Fig. 2A). The endothelial lining had been destroyed but the pattern of smooth muscle stretched around its perimeter was, in our view, diagnostic of a dilated vein and corresponds to one of the more rounded nodules seen in the gross specimen. The basic immunoprofile of the various tissue elements usefully highlighted the variability of the components from area to area (Fig. 2B). Typical adenomyotic foci were present in the lower (endocervical) surgical resection margin. However, intravascular extensions did not compromise the cervical margin or extend to the uterine serosa or the parametrial surgical plane of excision. The patient is presently asymptomatic and has a normal abdominopelvic computed tomography (CT) scan and chest X-ray. The management plan is to repeat these in 6 months time.

Anecdotal descriptions of endometrial tissue in myometrial vascular channels in association with adenomyosis date back almost 70 years[5] while subsequent published series have demonstrated involvement in 14 of 78 cases (17.9%) in one study,[6] 35 of 200 cases (17.5%) in another,[7] and more recently 54 of 434 cases (12.4%).[8] In most cases, as in ours, adenomyotic tissue was attached to the vessel wall and protruded into the vessel lumen beneath the endothelial lining. Contrasting with our case, however, in a significant majority of the examples in each of these studies[6−8] the intravascular component consisted of stroma only, under which circumstances low grade endometrial stromal sarcoma (LGESS) might legitimately enter the differential diagnosis. Typical differentiating features of adenomyosis, however, are the blandness of the stromal and glandular elements, absence of a tumour mass on gross examination,[8] or unequivocal areas of infiltrative neoplasm. Extrauterine extensions, when present, help to confirm LGESS. The presence of endometrial type glands, especially when prominent as in our case, clearly favours adenomyosis, even though these may occasionally be seen in LGESS,[9,10] as may smooth muscle.[11,12] The pattern of vascular involvement suggests to some authors[8] that